# ASSESSMENT OF AN INTERFACIAL SHEAR TERM FOR ADIABATIC DISPERSED AIR-WATER TWO-PHASE FLOW WITH THE TWO-FLUID MODEL

**S. L. Sharma, T. Hibiki, M. Ishii**
School of Nuclear Engineering, Purdue University
400 Central Dr., West Lafayette, IN 47907-2017, USA
sharma55@purdue.edu, hibiki@purdue.edu, ishii@purdue.edu

**J.P. Schlegel**
Nuclear Engineering Program, Missouri University of Science and Technology
301 W 14th St, Rolla, MO 65409, USA
schlegelj@mst.edu

**J.R. Buchanan, Jr., K. J. Hogan**
Bechtel Marine Propulsion Corporation, Bettis Laboratory
814 Pittsburgh-McKeesport Blvd, West Mifflin, PA 15122, USA
jack.buchanan@unnpp.gov, kevin.hogan@unnpp.gov

**P.W. Guilbert**
ANSYS UK Ltd
Milton Park, Abingdon, Oxfordshire, OX14 4SA,UK
paul.guilbert@ansys.com

## ABSTRACT

In commercially available Computational Fluid Dynamics (CFD) codes such as ANSYS CFX and Fluent, the interfacial shear term is missing in the field momentum equations. The derivation of the two-fluid model (Ishii and Hibiki, 2011) indicates the presence of this term as a momentum source in the right hand side of the field momentum equation. The inclusion of this term is considered important for proper modeling of the interfacial momentum coupling between phases. For separated flows, such as annular flow, the importance of the shear term is understood in the one-dimensional (1-D) form as the major mechanism by which the wall shear is transferred to the gas phase (Mishima and Ishii, 1984). For dispersed two-phase flow CFD simulations it is important to assess the significance of this term in the prediction of phase distributions. In the first part of this work, the closure of this term in three-dimensional (3-D) form in a CFD code is investigated. For dispersed gas-liquid flow, such as bubbly or churn-turbulent flow, bubbles are dispersed in the shear layer of the continuous phase. The continuous phase shear stress is mainly due to the presence of the wall and the modeling of turbulence through the Boussinesq hypothesis. In a 3-D simulation, the continuous phase shear stress can be calculated from the continuous fluid velocity gradient, so that the interfacial shear term can be closed using the local values of the volume fraction and the total stress of liquid phase. This form also assures that the term acts as an action-reaction force for multiple phases. In the second part of this work, the effect of this term on the volume fraction distribution is investigated. For testing the model two-phase flow data measured at Purdue University is assessed. The interfacial shear term is assembled in ANSYS CFX. Simulation results are presented to assess the effect of the interfacial shear term on the phase distribution.

**KEYWORDS**

Two-fluid model, Interfacial shear, CFD, Dispersed gas-liquid flow

## 1. INTRODUCTION

In recent years, CFD has emerged as a very useful tool for engineers and scientists, providing valuable information on the temporal and spatial distribution of key variables in a flow field. Most commercial CFD codes can be applied with confidence to solve a variety of single-phase flow problems; however, considerable research effort is still necessary before CFD can be applied to the study of gas-liquid two-phase flows with the same level of confidence. While Direct Numerical Simulation (DNS) is impractical for industrial flow problems involving significant void fraction, an Eulerian-Eulerian approach (two-fluid model) is widely used and considered well suited for industrial scale two-phase flow problems [1]. Present commercial two-phase CFD tools already have Eulerian-Eulerian modeling capability using the two-fluid model, which was developed by Ishii [1-3] by time averaging the instantaneous transport equations (continuity, momentum, and energy) for each phase. This time averaging results in interfacial transfer terms in the two-fluid model which require closure relations. The predictive capability of the two-fluid model relies heavily on the accuracy of these closure relations. In the present work, the focus is on adiabatic bubbly gas-liquid flow. In case of adiabatic two-phase flow, the three dimensional formulations of two-fluid model rigorously derived by Ishii [1,2] can be simplified as

Continuity equation:

$$\frac{\partial \alpha_k \rho_k}{\partial t} + \nabla \cdot \left( \alpha_k \rho_k v_k \right) = \Gamma_k ; \tag{1}$$

Momentum equation:

$$\frac{\partial \alpha_k \rho_k v_k}{\partial t} + \nabla \cdot \left( \alpha_k \rho_k v_k v_k \right) = -\alpha_k \nabla p_k + \nabla \cdot \alpha_k \left( \bar{\bar{\tau}} + \tau_k^t \right) \tag{2}$$

$$+ \alpha_k \rho_k g + v_{ki} \Gamma_k + M_{ik} - \nabla \alpha_k \cdot \tau_{ki} ;$$

where the subscript $i$ stands for the values at the interface; $\Gamma_k$ is the mass generation term; $M_{ik}$ is the interfacial force term; and $\tau_{ki}$ is the interfacial shear stress. The interfacial force terms in the momentum equation are generally considered to include a drag, lift, wall, and dispersion force for bubbles by liquid eddies. A thorough literature survey has been done to determine the best available hydrodynamic models for each of the forces. The best available models chosen and used for the current simulations are listed in Table I.

It is important to mention here that for some cases, especially those with high liquid velocity, some of the model coefficients were modified. Of specific concern was the lift force coefficient, which was changed to capture the void fraction trend seen in the measurements. This was done to isolate the effects of the interfacial shear term from other modeling uncertainties and will be discussed in a later section of the paper.

The interfacial shear term, $(-\nabla \alpha_k \cdot \tau_i)$, appears in the two-fluid model [1], but is missing in presently available commercial CFD codes. The term arises in the macroscopic interfacial momentum transfer development of the two fluid model. Whereas most of the drag and non-drag terms that comprise $M_{ik}$

arise from the normal components of the macroscopic interfacial momentum transfer, the interfacial shear comes from the tangential components. For this reason, most one-dimensional treatments developed for two-phase flow neglect the interfacial shear term unless considering either annular flow or horizontal flows [3]. As such, the interfacial shear is included in satisfying the macroscopic jump conditions when summed across all phases and fields. For three-dimensional treatments, it is important to implement the interfacial shear term and assess its significance.

**Table I. Summary of Interfacial Forces and Constitutive Relations for Momentum Equation Applied in Benchmark Cases**

| Interfacial Forces | Phases | Nature | Coefficient |
|---|---|---|---|
| Drag Force | Gas and Liquid | Interfacial force | Ishii and Zuber (1979) [5] |
| Wall Lubrication Force | Gas and Liquid | Interfacial force | Antal et al. (1991) [6] $C_{W1} = -0.01, C_{W2} = 0.05$ |
| Lift force | Gas and Liquid | Interfacial force | Hibiki and Ishii (2007) [7] |
| Turbulent dispersion force | Gas and Liquid | Interfacial force | Bertodano (1992) [8] $C_{TD,1} = 0.1$ |
| Bubble-induced turbulence | Liquid | Reynolds stress | Sato et al. (1981) [9] $C_{Sato,G1} = 0.6$ |

## 2. INTERFACIAL SHEAR TERM CLOSURE

The field momentum equations in CFX do not include the interfacial shear term ($-\nabla\alpha_k \cdot \tau_{ki}$). The inclusion of this term is important for proper modeling of the interfacial momentum coupling between phases [1,3]. This can be explained by considering the momentum equations for each phase and simplifying them in an area-averaged form.

*Gas phase:*
For the gas phase, several simplifications can be used. For example, due to the relatively small viscosity and density of the gas phase compared with the liquid phase, the total shear and gravitational terms can be neglected.

3-D form

$$\begin{aligned} &= -\alpha_g \nabla p + \nabla \cdot \left(\alpha_g \tau_g^T\right) + \alpha_g \rho_g \vec{g} + \overrightarrow{M}_{ig} - \nabla \alpha_g \cdot \overline{\overline{\tau}}_{gi} \\ &= -\alpha_g \nabla p + \overrightarrow{M}_{ig} - \nabla \alpha_g \cdot \overline{\overline{\tau}}_f^T \end{aligned} \tag{3}$$

1-D form

$$\begin{aligned} &= -\left\langle \alpha_g \frac{dp}{dz} \right\rangle + \left\langle \overrightarrow{M}_{ig}{}^D \right\rangle - \left\langle \nabla \alpha_g \cdot \overline{\overline{\tau}}_f^T \right\rangle_z \\ &= -\left\langle \alpha_g \right\rangle \left\langle \frac{dp}{dz} \right\rangle + \left\langle \overrightarrow{M}_{ig}{}^D \right\rangle - \left\langle \nabla \alpha_g \cdot \overline{\overline{\tau}}_f^T \right\rangle_z \end{aligned} \tag{4}$$

*Liquid phase:*
3-D form

$$= -\alpha_f \nabla p + \nabla \cdot \left( \alpha_f \tau_f^T \right) + \alpha_f \rho_f \vec{g} + \overline{\vec{M}}_{if} - \nabla \alpha_f \cdot \overline{\overline{\tau}}_{fi} \tag{5}$$

1-D form

$$= -\left\langle \alpha_f \frac{dp}{dz} \right\rangle + \left\langle \overline{\vec{M}}_{if}^{\,D} \right\rangle - \left\langle \nabla \cdot \left( \alpha_f \overline{\overline{\tau}}_f^{\,T} \right) \right\rangle_z + \left\langle \alpha_f \right\rangle \rho_f \vec{g} - \left\langle \nabla \alpha_f \cdot \overline{\overline{\tau}}_f^{\,T} \right\rangle_z \tag{6}$$

$$= -\left\langle 1 - \alpha_g \right\rangle \left\langle \frac{dp}{dz} \right\rangle + \left\langle \overline{\vec{M}}_{if}^{\,D} \right\rangle - \frac{4\tau_w}{D} + \left\langle \alpha_f \right\rangle \rho_f \vec{g} - \left\langle \nabla \alpha_f \cdot \overline{\overline{\tau}}_f^{\,T} \right\rangle_z$$

It is then important to understand how the interfacial shear term can be closed. Since the bubbles are dispersed in the continuous phase shear layer, the interfacial shear stress can be approximated by the continuous phase shear stress,

$$\tau_{ki} \approx \tau_f^T = \tau_f^\mu + \tau_f^t \tag{7}$$

$$-\nabla \alpha_{g1} \cdot \tau_{g1i} \approx \nabla \alpha_{g1} \cdot \left( \tau_f^\mu + \tau_f^t \right) \tag{8}$$

$$-\nabla \alpha_{g2} \cdot \tau_{g1i} \approx \nabla \alpha_{g2} \cdot \left( \tau_f^\mu + \tau_f^t \right) \tag{9}$$

$$-\nabla \alpha_f \cdot \tau_{fi} \approx \nabla \alpha_f \cdot \left( \tau_f^\mu + \tau_f^t \right) \tag{10}$$

The above form also assures that this term acts as an action-reaction force for the phases such that:

$$-\nabla \alpha_{g1} \cdot \tau_{g1i} - \nabla \alpha_{g2} \cdot \tau_{g2i} - \nabla \alpha_f \cdot \tau_{fi} = 0 \tag{11}$$

This term should be included in the field momentum equation of CFD codes because this term becomes very important in separated flows such as annular flows or horizontal stratified flows. This is due to the very high void gradients across the interface between the separated phases.

To illustrate the importance of the interfacial shear term, it is useful to show how the one-dimensional form of the term evolves through various flow regimes. In the case of annular two phase flow in a tube, the one-dimensional (area averaged) axial contribution becomes

$$\left\langle \left( \nabla \alpha_g \right) . \tau_i \right\rangle_z = -\frac{1}{A} \int_0^R \frac{\partial \alpha}{\partial r} \tau_i (2\pi r dr) = -\frac{1}{\pi R^2} \lim_{\delta \to 0} \int_\delta \frac{\partial \alpha}{\partial r} \tau_i (2\pi r dr) = -\frac{P_i}{A} \tau_i , \tag{12}$$

where $P_i$ is the interfacial wetted perimeter of the gas core. Here, $\tau_i$ is generally closed through constitutive relations in terms of an interfacial friction factor such as the Wallis correlation [10] for a rough, wavy film.

In the case of dispersed gas-liquid flow, the continuous phase shear stress is mainly due to the presence of the wall. In a 3-D simulation in CFX, the continuous phase shear stress can be calculated from the velocity gradient, so that the interfacial shear term can be closed using the local value of the void gradient and liquid phase total stress term given in equations (7) through (11). Again, it will be useful to understand how these terms can be closed in an area-averaged two-fluid model formulation, especially for dispersed flow regimes like bubbly or churn-turbulent flow. In its one-dimensional form, the constitutive relation in the dispersed phase requires the void and shear stress distribution. A power law distribution for shear stress and void fraction is assumed such that

$$\tau_i = \tau_w \left(\frac{r}{R}\right)^m, \frac{\alpha_k - \alpha_{kw}}{\alpha_{ko} - \alpha_{kw}} = 1 - \left(\frac{r}{R}\right)^n \tag{13}$$

$$-\left\langle \left(\nabla \alpha_g\right).\tau_i \right\rangle_z = -\frac{1}{A}\int_0^R \frac{\partial \alpha}{\partial r}\tau_i (2\pi r dr) = -\frac{n+2}{n+m+1}\left\langle \alpha_g \right\rangle \frac{4\tau_w}{D}, \tag{14}$$

where $C_\tau = \frac{n+2}{n+m+1}$ is the distribution parameter. The value of *m* is theoretically equal to unity in the case of single phase flow. If it is assumed it to be close to unity for two-phase flow then $C_\tau$ can be expected to be close to unity. This gives the closure in one dimensional form for the shear term as

$$-\left\langle \left(\nabla \alpha_g\right).\tau_i \right\rangle_z \cong -\left\langle \alpha_g \right\rangle \frac{4\tau_w}{D} \tag{15}$$

In a horizontal channel this term will contribute to the slip between the dispersed and continuous phases even under a steady state conditions. The inclusion of this term does not alter the overall momentum balance of a two phase mixture because of the macroscopic momentum jump condition. However it indicates that the momentum interaction between phases is affected by the wall shear stress through the interfacial shear and void gradient distributions [2,3]. So in one-dimensional form, the right hand side (R.H.S.) of field momentum equations (M.E.) are:

R.H.S.of Gas M.E.

$$= -\left\langle \alpha_g \right\rangle \left\langle \frac{dp}{dz} \right\rangle - \frac{4\left\langle \alpha_g \right\rangle \tau_W}{D} + \left\langle \overline{M}_{ig}{}^D \right\rangle \tag{16}$$

R.H.S.of Liquid M.E.

$$= -\left(1 - \left\langle \alpha_g \right\rangle\right)\left\langle \frac{dp}{dz} \right\rangle - \frac{4\left(1 - \left\langle \alpha_g \right\rangle\right)\tau_w}{D} + \left\langle \alpha_f \right\rangle \rho_f \bar{g} + \left\langle \overline{M}_{if}{}^D \right\rangle \tag{17}$$

It can be seen that for the gas phase, the presence of wall is felt through this interfacial shear term.

In the present work, an attempt is made to assess the importance of this term in the 3-D form of the phase distribution in a cross-section for dispersed two-phase flow. The missing interfacial shear term in CFX is calculated in a 3-D form for each phase from the product of the continuous phase total stress term and the volume fraction gradient of the respective phase. This term is then added implicitly to the respective phase momentum equation to account for the importance of this term and its effect on the phase distribution for dispersed flow. The continuous phase total stress is calculated from a Boussinesq hypothesis using the velocity gradient.

For the assessment of the interfacial shear term, adiabatic upward bubbly air-water two-phase flow data measured in two different geometries at Purdue University are utilized. The first test section is of narrow rectangular geometry with cross-sectional dimension of 200mm (x-direction) by 10mm (y-direction) and was approximately 3m in height [4]. The second geometry considered is a round tube with an inner diameter of 50.8 mm and 3.061m length [11]. Conductivity probe ports were installed at three locations along the flow duct length to measure the local two phase parameters such as void fraction, interfacial area concentration, and gas velocity. In the case of the rectangular channel, probes were located at $z/D_H$ =35, 88 and 142 away from inlet. In the case of the pipe geometry the probes were installed at $z/D_H$ =6, 30.3 and 53.5. Uniform injection method for gas and liquid was used at the inlet. Further details of the test facilities are presented in more detail by Kim [4] and Hibiki et al. [11]. The flow conditions for the database used in this study are summarized in Table II and Figure 1.

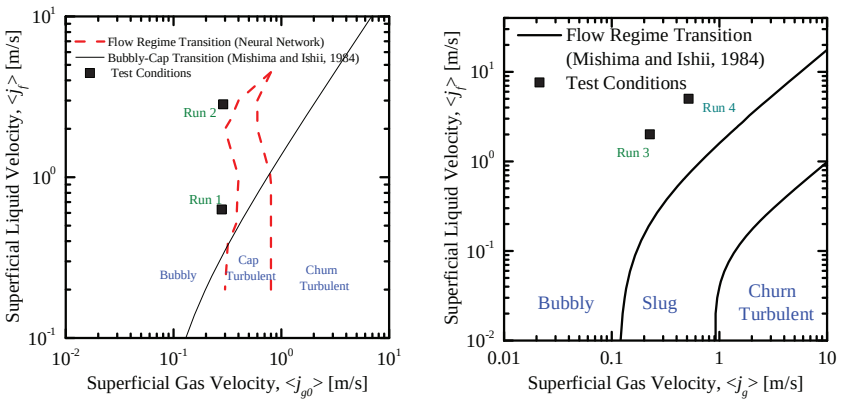


**(a)** **(b)**

**Figure 1. Test conditions in a $j_g$–$j_f$ map for (a) Narrow Rectangular channel [4] and (b) Pipe [11].**

**Table II. Summary of Test Conditions**

| Run 1 | Run 2 | Run 3 | Run 4 |
|---|---|---|---|
| <$j_{g,0}$>=0.28 m/s<br><$j_f$>=0.63 m/s | <$j_{g,0}$>=0.29 m/s<br><$j_f$>=2.84 m/s | <$j_{g,0}$>=0.226 m/s<br><$j_f$>=2.01 m/s | <$j_{g,0}$>=0.518 m/s<br><$j_f$>=5 m/s |
| Rectagular channel 200mm x 10mm | Rectagular channel 200mm x 10mm | Pipe, 50.8mm ID | Pipe, 50.8mm ID |

## 3. PREPARATION OF THE BENCHMARK

The preparation of the benchmark starts with the geometry and mesh generation. The first geometry is a rectangular duct that has dimensions of $200\text{mm} \times 10\text{mm} \times 2340\text{mm}$. The domain is focused on one-quarter of the duct cross-section as shown in Figure 2. This was selected to save computational time based on assumed symmetric conditions. Based on a mesh sensitivity study it was found that hexahedral mesh configuration of $60 \times 10 \times 162$, with a total of 97,200 computational cells, was sufficient to give details of the phase distribution in the present geometry. A mesh with relatively fine cells near the wall region is used to capture the high gradient of two-phase flow parameters near the wall. While selecting the mesh size near the wall, it was ensured that the value of $y^+$ is greater than 30 for first the first node, as the law of the wall has been used for the present simulation.

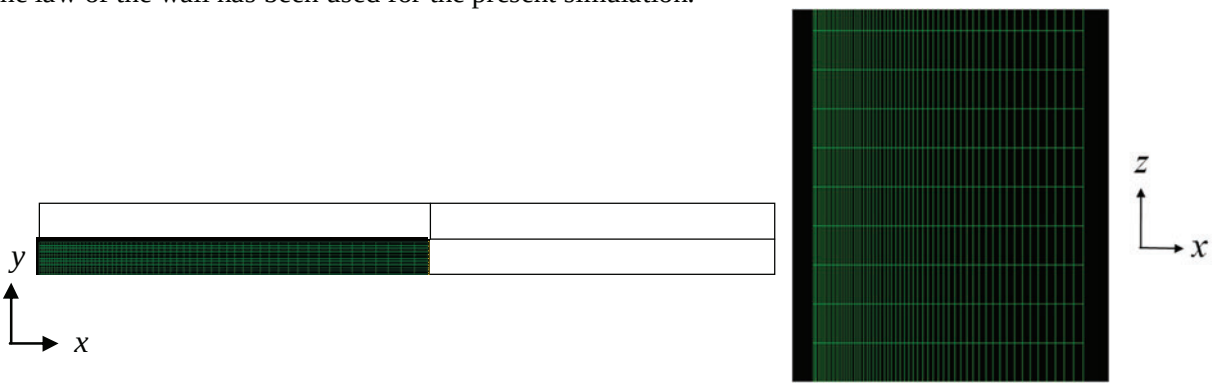


**(a)Transverse Mesh** **(b) Axial Mesh**

**Figure 2. Mesh used for Flow Conditions for Rectangular Channel Geometry**

The second case is a pipe geometry. A two degree azimuthal wedge with a radius of 25.4mm is considered with symmetry assumed in the azimuthal direction. After a grid sensitivity analysis, 36 nodes in the radial direction and 130 uniform nodes in the axial direction were found to be sufficient to capture the physics and satisfy the requirement for the wall function approach (Figure 3).

**Figure 3. Cross section of Mesh used for Pipe Geometry**

The inlet boundary conditions are based on information at the first measurement location. This is port 2, $z/D_H$ =35, in the rectangular channel and port 1, $z/D_H$ =6, in the case of the pipe. The local measurements of void fraction and gas velocity are used to specify the inlet boundary conditions and domain initialization. For the rectangular channel, the liquid velocity profile is derived from the gas velocity profile by subtracting the slip velocity. In the short gap direction, or *y*-direction, a $1/7^{th}$ power law variation is assumed for the liquid velocity profile. In the case of the pipe the liquid velocity profile was also measured at port 1 and was used as the inlet condition. A constant relative pressure of 0 Pa is used for the outlet boundary condition for both cases. A free slip wall boundary condition is specified for the gas phase, with a no slip wall boundary condition for the liquid phase. However, the scalable wall function is applied for the treatment of liquid flow near the wall [12]. The $k-\varepsilon$ turbulence model is used for the turbulence model [13- 23].

In the current benchmark study ANSYS CFX-15.0 with a new customized executable solver has been used for three-field two-fluid model simulations. The three fields include the liquid phase and two gas fields for a two-bubble-group approach. "High Resolution" is selected as the advection scheme and $10^{-5}$ is taken as the Root Mean Square (RMS) residual target for convergence of the simulation. The coupled void fraction option under "Multiphase Control" options has been used in the simulations. The time step for run was selected on a case-by-case basis to obtain faster convergence.

## 4. RESULTS AND DISCUSSION

### 4.1. Run 1

Run 1 belongs to a bubbly flow condition with relatively low liquid and gas velocities, as shown in Fig. 1(a). The liquid and gas phase were injected uniformly at the inlet. The void fraction profile at port 2 which was used as the boundary condition is mostly uniform, but does contain features from the injection spargers, as seen in Figure 4. The local phase distribution prediction without the interfacial shear term is compared with the measurements at port 4 and port 6. The figure shows the local prediction of void fraction along the line $y$ = 1mm, which is near the wall, and at $y$ = 5mm, along the centerline. The prediction shows typical bubbly flow wall-peaking phenomenon. The variation in the *y*-direction along the lines $x$ = 3mm, which is near the wall, and $x$ = 100 mm, which is the centerline, shows that the overall trend of the void fraction distribution in *y*-direction is fairly well predicted by CFX.

Figure 5 shows the effect of addition of the interfacial shear term (IAS) in the field momentum equation. As can been seen from phase distribution plot, the effect is mostly limited to the near-wall region. This is expected, as both interfacial shear and void gradient is expected to be high near the wall region. After addition of the IAS, the void fraction is redistributed away from wall. This is most notable in the y=1mm line and confirmed in the x=3mm and y=90mm lines in Figure 5.

### 4.2. Run 2

The second case to be discussed here belongs to a finely dispersed bubbly flow. This case is at relatively high liquid velocity ($j_f$=2.84 m/s). For this case, measurement data are only available for ports 2 and 6. First, the simulation was carried out with the interfacial force models included in the Table I, without the IAS. It was found that most of the bubbles were swept to the near-wall region by the lift force, which created a physically unrealistic void profile. The physics-based lift coefficient model of Hibiki and Ishii was originally benchmarked with experimental data for mainly low liquid velocity conditions [7]. At high liquid flow rates, the effect of turbulence on the lift coefficient in the presence of wall region has not been understood clearly in literature. Investigations of this effect are not in the scope of the present work. Therefore, the lift coefficient was lowered to 0.05 to reproduce the measured void fraction profile at port 6 for this highly turbulent bubbly flow case. Since it is difficult to predict the trend at all locations of the domain, the center lines ($y$ = 5mm, $x$ = 90mm) were targeted. The local phase distribution results with a lift coefficient of 0.05 show good prediction in both wide ($W$ = 200mm) and narrow ($G$ = 10mm) directions as shown in Figure 6. The effect of addition of the IAS on the local void fraction distribution is shown in Figure 7. The effect of the addition of the interfacial shear term is limited to the near wall region.

The two cases discussed previously belong to the rectangular channel geometry, where three dimensional effects were present. However, to see strictly two dimensional effects, two-phase flow data measured in a 50.8mm ID pipe geometry was used for a second assessment.

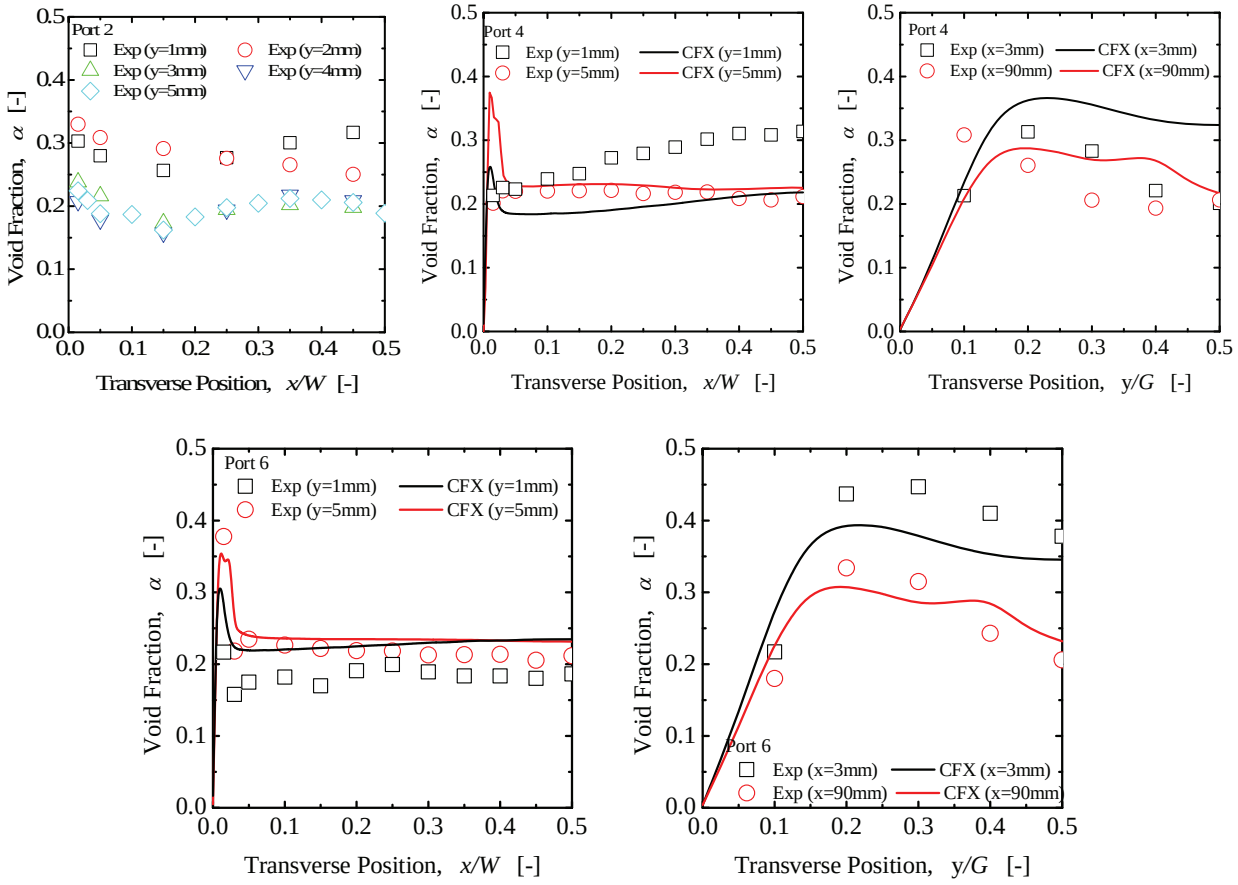


**Figure 4. Local phase distribution at Port 2, 4 and 6 (Run 1)**

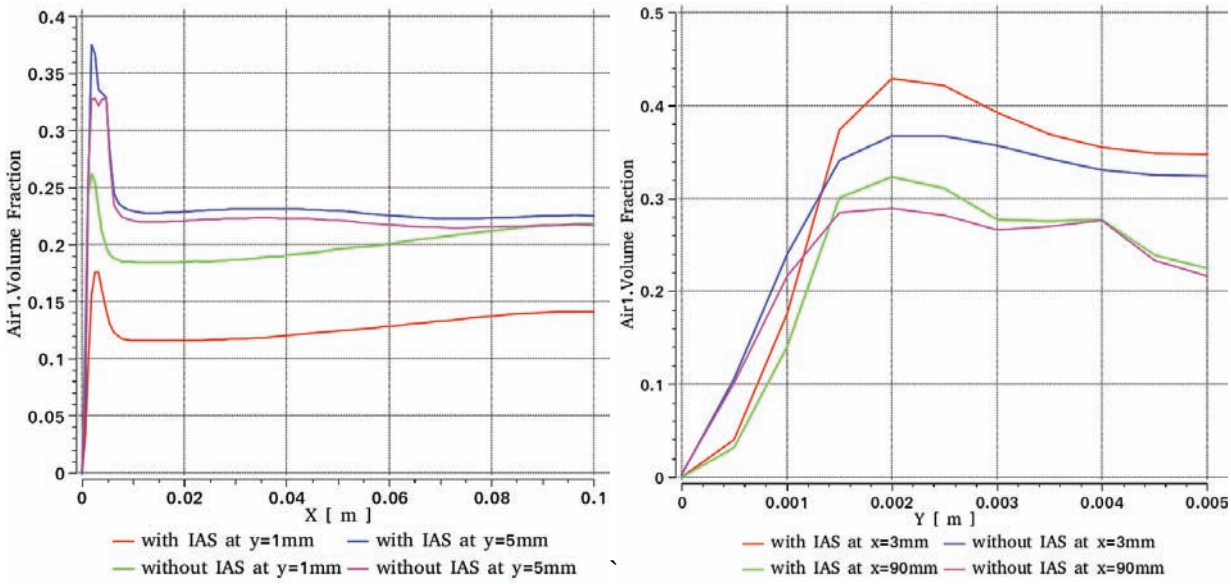


**(a)**

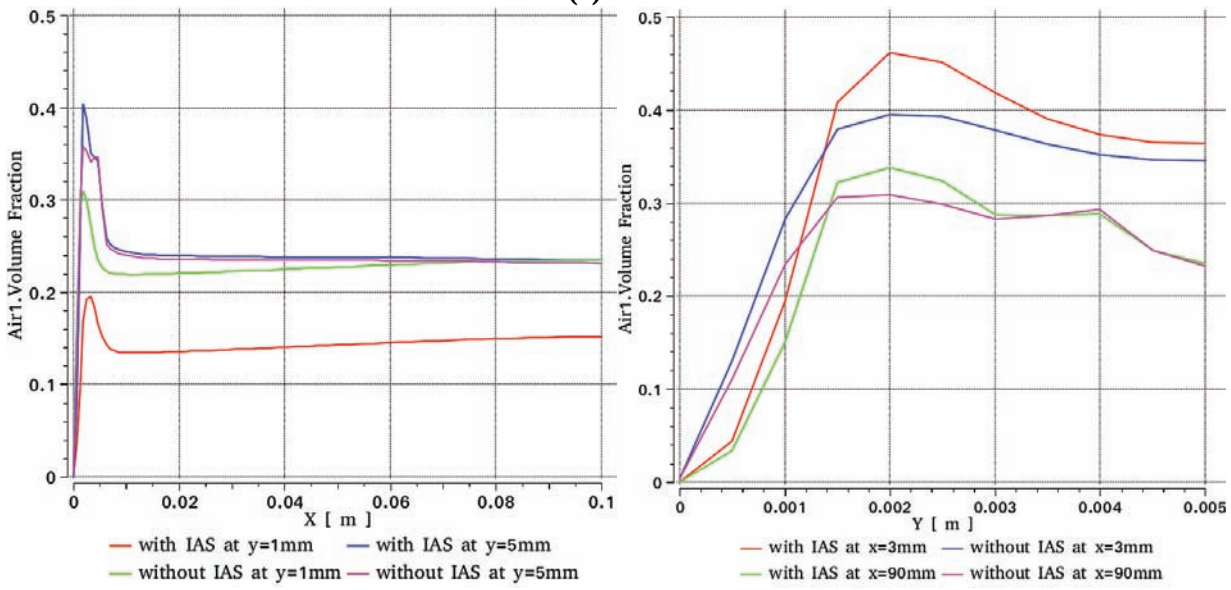


**(b)**

**Figure 5. Local phase distribution at (a) Port 4 and (b) Port 6 with and without addition of interfacial shear term IAS (Run 1)**

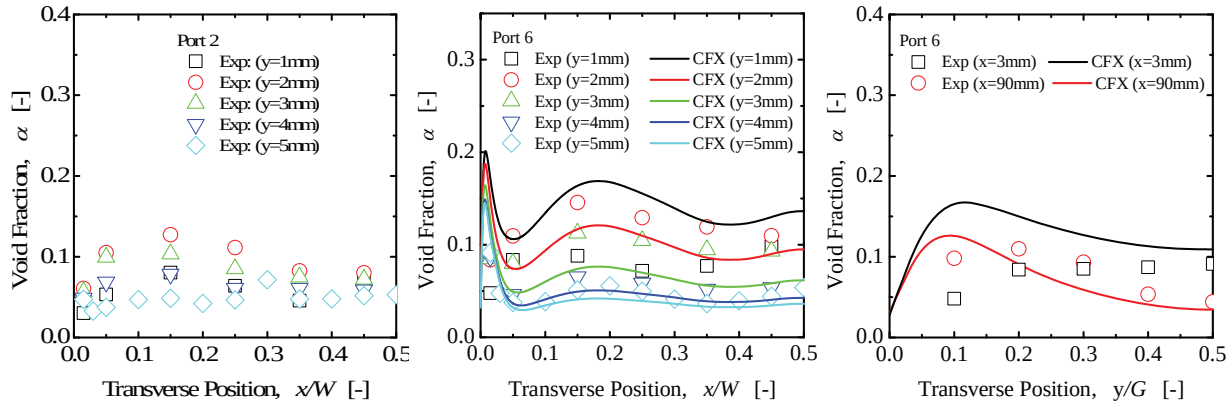


**Figure 6. Local phase distribution at Port 6 (Run 2)**

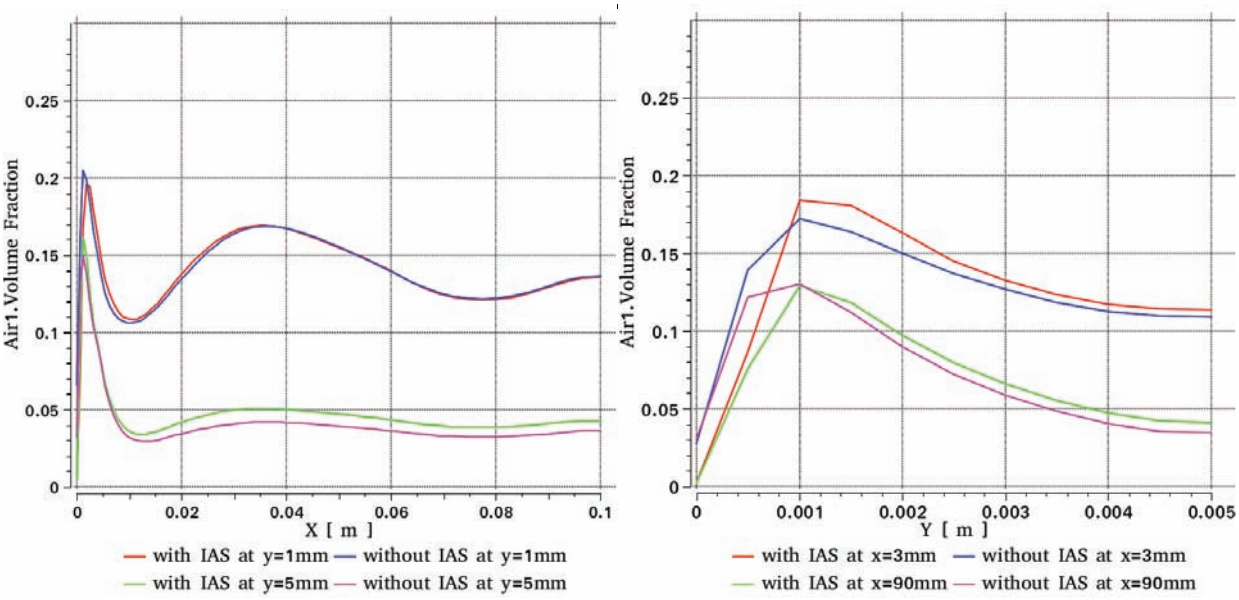


**Figure 7. Local phase distribution at Port 6 with and without addition of interfacial shear term (Run 2)**

### 4.3. Run 3

For Run 3, the initial simulation with the set of interfacial forces included in Table I showed significantly high wall peaking profile as shown Figure 8. The physics based lift coefficient model of Hibiki and Ishii [7] (using a lift coefficient of 0.39 for this case) caused all bubbles to move towards the wall. This trend was not seen in the measurements at Port 2 and Port 3. This is a relatively high liquid velocity case ($j_f$=2m/s). Turbulence may have effect on the lift coefficient. The lift coefficient was simply reduced to match the void profile seen in the measurements, as the main objective of the task was to see the effect of addition of the interfacial shear term. A lift coefficient of 0.04 gave a void profile similar to that seen in the measurements. This case was then run with the IAS implemented. Figure 9 shows, at both port 2 and 3, that the addition of the term has small effect on the void profile and is limited to near wall region.

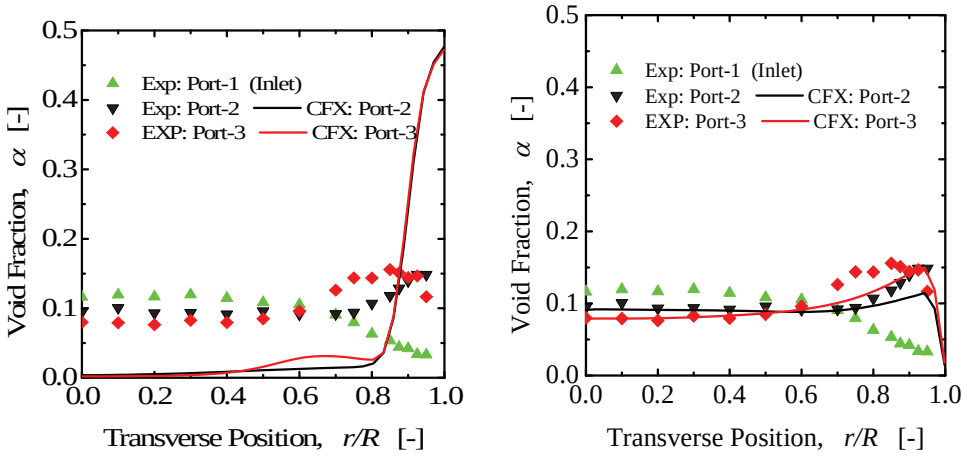


**(a)** **(b)**

**Figure 8. Local Phase Distribution at Port 1, 2, and 3 with (a) Hibiki-Ishii lift coefficient model, lift Coefficient=0.39 (b) with Lift Coefficient=0.04 (Run 3)**

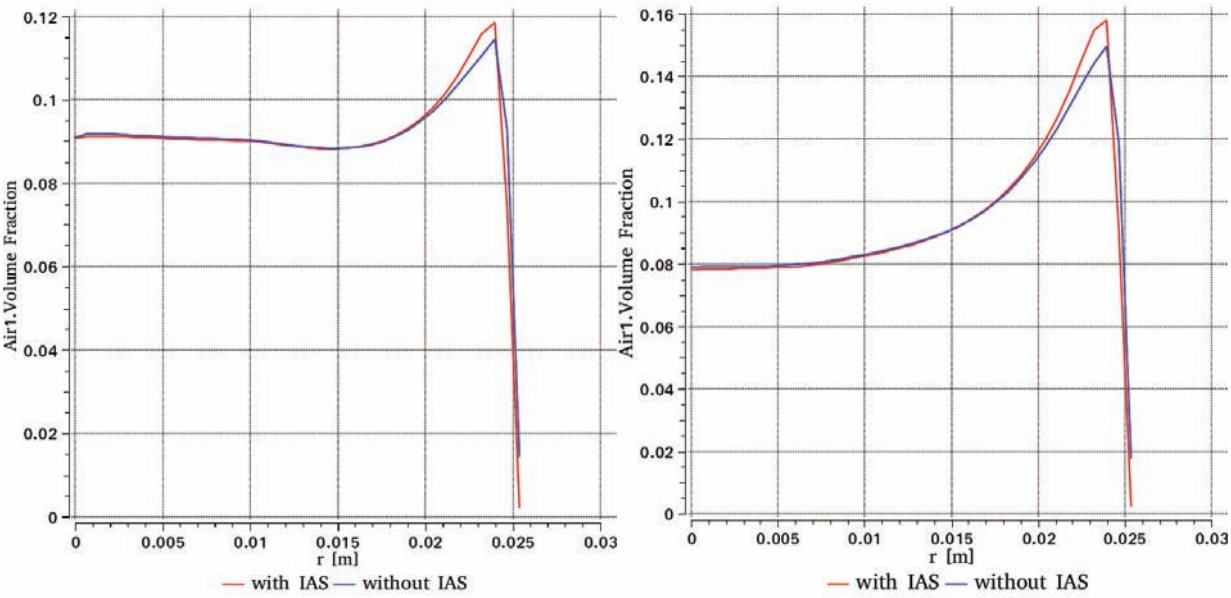


**(a)** **(b)**

**Figure 9. Local Phase Distribution at (a)Port 2 and (b) Port 3, with and without addition of interfacial shear term (Run 3)**

### 4.4. Run 4

The last case which will be discussed here is Run 4, which is a finely dispersed bubbly flow at relatively high liquid flow rate. The void distribution results with the Hibiki and Ishii [7] lift force coefficient model (lift coefficient ~ 0.47) predicted very high void fraction near the wall region (Figure 10(a)), i.e. all bubbles were moved to the near-wall region by the lift force, which was not seen in the experimental data. Therefore the lift coefficient was reduced to 0.01 to match the measured void fraction profile trend. As can be seen from Figure 10(b) the void fraction then matched the trend. After addition of the IAS, the volume fraction is redistributed away from wall. However, overall only slight differences were seen in the void distribution at port 2 and 3 near the wall region as shown in Figure 11.

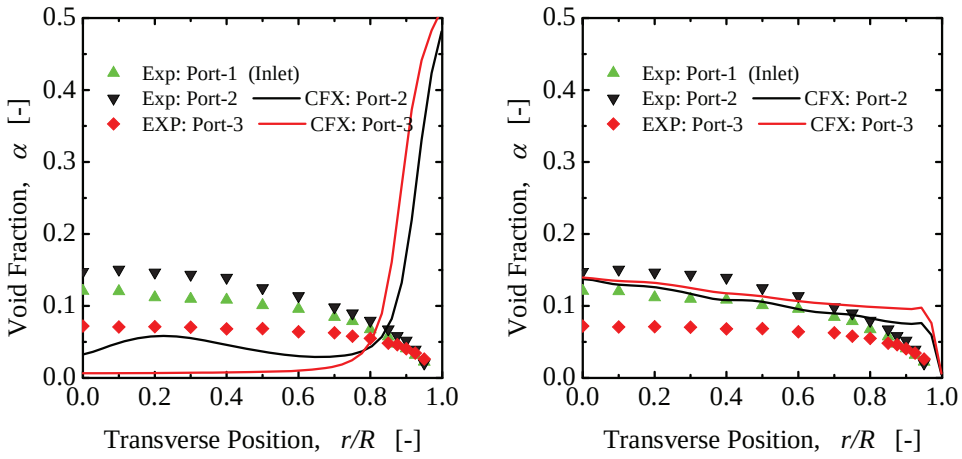


**(a)** **(b)**

**Figure 10. Local phase distribution at Port 1,2 and 3 with (a) Hibiki-Ishii Lift Coefficient Model, Lift coefficient=0.47 (b) Lift coefficient=0.01 (Run 4)**

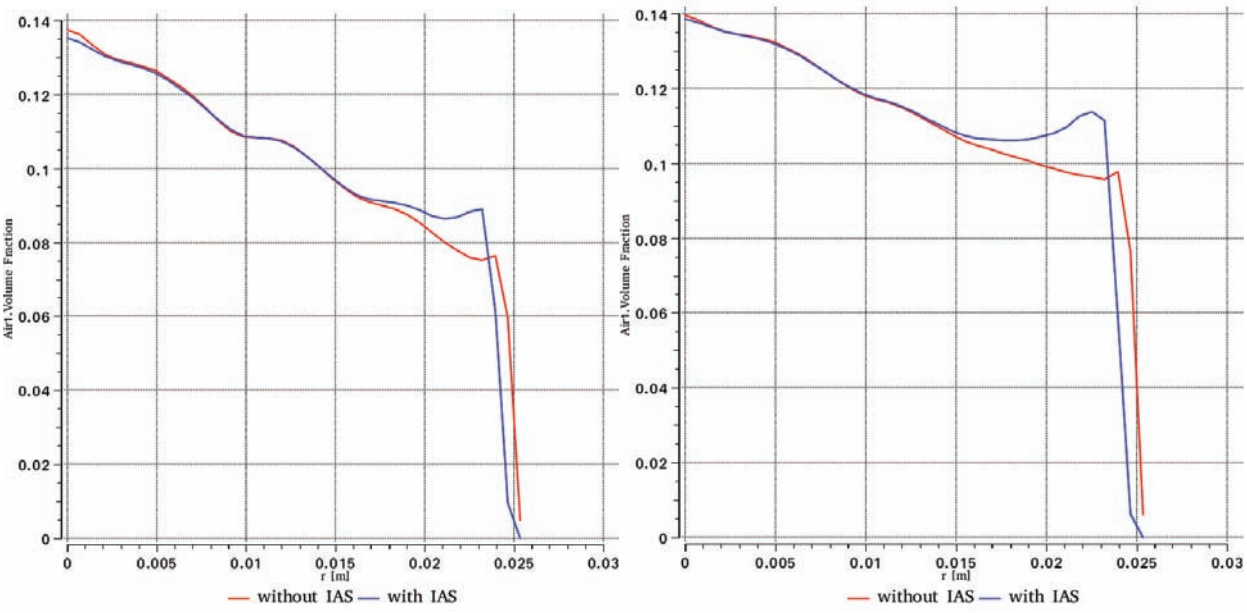


**(a)** **(b)**

**Figure 11. Local phase distribution at (a) Port 2 and (b) Port 3 with and without Addition of interfacial shear term (Run 4)**

## 5. CONCLUSION

A CFD model was prepared for assessing the interfacial shear term ($-\nabla\alpha_k \cdot \tau_i$) within the framework of ANSYS CFX for rectangular channel and pipe geometries. Benchmark simulations against adiabatic air-water upward bubbly flow data were carried out with applicable interfacial forces including drag, lift, and bubble dispersion force. Sato's model [9] was used for modeling bubble-induced turbulence for the liquid phase. The main conclusions from this effort are

1. For the higher liquid flow rate cases analyzed here the lift coefficient had to be reduced significantly in order to reproduce the measured void profile. The possible effect of turbulence on lift coefficient at high liquid flow rate has not been significantly investigated in the literature and this effect should be addressed in future research.
2. The addition of the interfacial shear term ( $-\nabla\alpha_k \cdot \tau_{ki}$ ) resulted in small effects limited to the near-wall region, as the continuous phase stress is high in this region.
3. Additional cases with higher void fractions need to be assessed in near future, as the interfacial shear term is expected to have more influence under those conditions.

## Notice



## REFERENCES

1. M. Ishii and T. Hibiki,. *Thermo-fluid dynamics of two-phase flow*.2nd Ed., Springer, New York (2011).
2. M. Ishii., *Thermo-fluid dynamic theory of two-phase flow*. Eyrolles, Paris (1975).
3. M. Ishii and K. Mishima, "Two-fluid model and hydrodynamic constitutive relations". *Nucl. Eng. Des*. **82**, pp. 107-126 (1984).
4. S. Kim, *Interfacial area transport equation and measurement of local interfacial characteristics*, Ph.D. Thesis, Purdue University, West Lafayette, IN (1999).
5. M. Ishii and N. Zuber, "Drag coefficient and relative velocity in bubbly, droplet or particulate flows". *AIChE J.* **25**, pp.843 (1979).
6. S. P. Antal, R. T. Lahey Jr., and J. E. Flaherty, "Analysis of phase distribution in fully developed laminar bubbly two-phase flow". *Int. J. Multiphase Flow* **17**, pp. 635-652 (1991).
7. T. Hibiki and M. Ishii, "Lift force in bubbly flow systems", *Chem. Eng. Sci*. **62**, pp. 6457-6474 (2007).
8. M. Lopez de Bertodano, *Turbulent Bubbly Flow in a Triangular Duct*, Ph.D. Thesis, Rensselaer Polytechnic Institute, Troy New York (1992).
9. Y. Sato, M. Sadatomi and K. Sekoguchi, "Momentum and heat transfer in two-phase bubble flow I", *Int. J. Multiphase Flow* **7**, pp. 167-177(1981).
10. G. B., Wallis, *One-dimensional Two-phase Flow*, McGraw-Hill Book Co.,USA (1969)
11. T. Hibiki, M. Ishii, Z. Xiao, Axial interfacial area transport of vertical bubbly flows. *Int. J. Heat Mass Transfer* **44**, 1869–1888 (2001).
12. ANSYS CFX Release 15.0, *ANSYS CFX-Solver Theory Guide*, ANSYS Inc.(2013)
13. M. A. Lopez de Bertodano, R. T. Lahey Jr, O. C. Jones, "Development of a $k-\varepsilon$ model for bubbly two-phase flow", *ASME J. Fluids Eng.* **116**, pp. 128-134 (1994).

14. A.A. Troshko, Y.A. Hassan, "A two-equation turbulence model of turbulent bubbly flows", *Int. J. Multiphase Flow* **27**(11), pp. 1965-2000 (2001).
15. E. Olmos, C. Gentric, C. Vial, G. Wild, and N. Midoux, "Numerical simulation of multiphase flow in bubble column reactors- influence of bubble coalescence and break-up" *Chem. Eng. Sci.* **56**, pp. 6359-6365 (2001).
16. V.V. Buwa, and V.V. Ranade. Dynamics of gas-liquid flow in a rectangular bubble column: experiments and single/multi-group CFD simulations. *Chem. Eng. Sci.* **57**, 4715-4736 (2002).
17. F. Lehr, M. Millies, D. Mewes, "Bubble-size distributions and flow fields in bubble columns", *AIChE J.* **48** (11), pp. 2426-2443 (2002).
18. E. Olmos, C. Gentric and N. Midoux, "Numerical description of flow regime transitions in bubble column reactors by a multiple gas phase model" *Chem. Eng. Sci.* **58**, 2113-2121 (2003).
19. T. Frank, J. Shi and A. D. Burns, "Validation of Eulerian multiphase flow models for nuclear safety applications" *Proc. 3rd International Symposium on Two-Phase Flow Modeling and Experimentation*. Pisa, Italy (2004).
20. D. Zhang, N.G. Deen and J.A.M. Kuipers, "Numerical simulation of the dynamic flow behavior in a bubble column: a study of closures for turbulence and interface forces" *Chem. Eng. Sci*. **61**, pp. 7593-7608 (2006).
21. Z. Sha, A. Laari, and I. Turunen, "Multi-phase-multi-size-group model for the inclusion of population balances into the CFD simulation of gas-liquid bubbly flows" *Chem. Eng. Technol*. **29**, pp. 550-559 (2006).
22. E. Krepper, B.N.R. Vanga, A. Zaruba, H.M. Prasser, and M.A. Lopez de Bertodano, "Experimental and numerical studies of void fraction distribution in rectangular bubble columns", *Nucl. Eng. Des*. **237**, pp. 399-408 (2007).
23. D. Prabhudharwadkar, C. Bailey, M.A. Lopez de Bertodano and J.R. Buchanan, "Two-Fluid CFD model of adiabatic air-water upward bubbly flow through a vertical pipe with a one-group interfacial area transport equation", *ASME 2009 Fluids Engineering Division Summer Meeting (FEDSM2009)*, Vail, Colorado, USA (2009).